BJR

■ **BONE BIOLOGY**

Auraptene ameliorates osteoporosis by inhibiting RANKL/NFATc1 pathway-mediated bone resorption based on network pharmacology and experimental evaluation

M. H. Kim,
L. Y. Choi,
J. Y. Chung,
E-J. Kim,
W. M. Yang

From Kyung Hee University, Seoul, South Korea

Aims

The association of auraptene (AUR), a 7-geranyloxycoumarin, on osteoporosis and its potential pathway was predicted by network pharmacology and confirmed in experimental osteoporotic mice.

Methods

The network of AUR was constructed and a potential pathway predicted by Kyoto Encyclopedia of Genes and Genomes (KEGG) pathway and Gene Ontology (GO) terms enrichment. Female ovariectomized (OVX) Institute of Cancer Research mice were intraperitoneally injected with 0.01, 0.1, and 1 mM AUR for four weeks. The bone mineral density (BMD) level was measured by dual-energy X-ray absorptiometry. The bone microstructure was determined by histomorphological changes in the femora. In addition, biochemical analysis of the serum and assessment of the messenger RNA (mRNA) levels of osteoclastic markers were performed.

Results

In total, 65.93% of the genes of the AUR network matched with osteoporosis-related genes. Osteoclast differentiation was predicted to be a potential pathway of AUR in osteoporosis. Based on the network pharmacology, the BMD and bone mineral content levels were significantly ($p < 0.05$) increased in the whole body, femur, tibia, and lumbar spine by AUR. AUR normalized the bone microstructure and the serum alkaline phosphatase (ALP), bone-specific alkaline phosphatase (bALP), osteocalcin, and calcium in comparison with the OVX group. In addition, AUR treatment reduced TRAP-positive osteoclasts and receptor activator of nuclear factor kappa-B ligand (RANKL)$^+$nuclear factor of activated T cells 1 (NFATc1)$^+$ expression in the femoral body. Moreover, the expressions of initiators for osteoclastic resorption and bone matrix degradation were significantly ($p < 0.05$) regulated by AUR in the lumbar spine of the osteoporotic mice.

Conclusion

AUR ameliorated bone loss by downregulating the RANKL/NFATc1 pathway, resulting in improvement of osteoporosis. In conclusion, AUR might be an ameliorative cure that alleviates bone loss in osteoporosis via inhibition of osteoclastic activity.

Cite this article: *Bone Joint Res* 2022;11(5):304–316.

Correspondence should be sent to Woong Mo Yang; email: wmyang@khu.ac.kr

Article focus

■ Investigation of the relevance of the possible effects and potential molecular pathways of AUR on osteoporosis using network pharmacology, and confirmation in an experimental osteoporotic mice model.

Key messages

- Auraptene (AUR), a 7-geranyloxycoumarin, is found in numerous edible fruits and vegetables such as the Rutaceae and Umbelliferae families, *Poncirus trifolia* and *Zanthoxylum piperitum*.
- A total of 65.93% of the target genes in the AUR network matched with osteoporosis-related genes, indicating that the potential effect of AUR is closely associated with osteoporosis.
- AUR increased the bone mineral density (BMD) level and serum biomarkers, and recovered the histological structure in osteoporotic mice.
- Based on the predicted pathway by network pharmacology, AUR ameliorated bone loss in osteoporosis by suppression of receptor activator of nuclear factor kappa-B ligand (RANKL)/nuclear factor of activated T cells 1 (NFATc1)-mediated osteoclast activities.

Strengths and limitations

- This is the first study to predict and confirm the efficacy and potential pathway of AUR on osteoporosis by network pharmacology and experimental evaluation.
- Further studies are needed to confirm the osteoporotic effects of AUR in humans.

Introduction

Osteoporosis is a systemic skeletal disorder that reduces bone mass and increases the risk of fracture due to deterioration of the microstructure of the bone tissue.[1] It occurs at the wrist, hip, vertebrae, and distal radius after minimal trauma.[2] Many patients suffer from pain, disturbance of physical function, reduction of social interactions, emotional problems, and financial burden for decades.[2,3] These characteristics reduce patients' quality of life, and for this reason osteoporosis is regarded as a major public health problem in an ageing society.[4] In over 200 million people in aged populations worldwide, at least 40% of elderly women are diagnosed with osteoporosis.[3] The most common diagnostic method for osteoporosis is to measure bone mineral density (BMD) using dual-energy X-ray absorptiometry (DXA).[5] According to the World Health Organization criteria, T-score measured in the lumbar spine and hip are classified and diagnosed as osteoporosis when the values are -2.5 or less.[6]

Low levels of vitamin D and calcium, ageing, and oestrogen deficiency are key parameters of increasing osteoporosis.[7] One of the aetiological factors of osteoporosis, especially in postmenopausal osteoporosis, is oestrogen deficiency, which accelerates bone turnover to increase bone resorption.[8] This leads to damaged bone tissue and bone breakdown, due to inhibition of osteoblast differentiation and induction of osteoclast apoptosis.[9] Osteoporosis caused by oestrogen deficiency can be treated with drugs such as bisphosphonates that suppress bone resorption, and selective oestrogen receptor modulators (SERMs), including raloxifene and tamoxifen, that improve bone formation through oestrogen activity.[7] However, these drugs may have side effects such as gastrointestinal disturbance, fever, breast cancer, heart failure, and osteonecrosis.[10,11] Therefore, finding new therapeutic reagents should be required for the treatment of osteoporosis more safely.

Auraptene (AUR), a 7-geranyloxycoumarin, is isolated from numerous edible fruits and vegetables such as the Rutaceae and Umbelliferae families, *Poncirus trifolia* and *Zanthoxylum piperitum*.[12] It is pharmacologically known to have anti-diabetes, anti-protozoal, anti-genotoxic, and anti-inflammation properties.[13] Recently, 5'-hydroxy auraptene, a coumarin derivative isolated from *Lotus lalambensis Schweinf*, was reported to promote osteoblast differentiation and inhibit osteoclast differentiation. Additionally, our previous research proved that the extracts of *Z. piperitum* have inhibitory effects against osteoclast differentiation in osteoporosis, suggesting the potential of AUR for osteoporosis.[14-16] In this study, we investigated the effects of AUR on bone loss with the underlying mechanism of osteoclast differentiation by network pharmacology and animal experiments.

Methods

Network construction of AUR and comparison of the osteoporosis gene set. To construct the network of AUR, genes related to AUR (Pubchem CID: 1550607) were collected through PubChem.[17] In total, 91 genes were shown as chemical-gene co-occurrences in the literature (Supplementary Table i) and created a network of AUR. Using GeneCards,[18] osteoporosis-related genes were extracted to create the osteoporosis gene set. They were found by searching "osteoporosis" as a keyword in the GeneCards database. The osteoporosis gene set consisted of a total of 4,576 genes. Each gene of the AUR network and osteoporosis gene set was counted, and the overlapping genes were sorted.

Functional enrichment analysis. Biological processes related to the targets of AUR were investigated using the Cytoscape String App (National Institute of General Medical Sciences, USA). The pathway terms categorized by the Kyoto Encyclopedia of Genes and Genomes (KEGG) Pathway Database and Gene Ontology (GO) Process were collected. Osteoporosis-related biological terms were selected, and the number of matching genes was counted.

Animal experiment. Five-week-old female Institute of Cancer Research (ICR) mice were housed in a controlled animal facility with 22°C ± 2°C of temperature, 50% ± 5% of humidity, light/dark cycle, and had free access to food and water for a week before the experiment. A total of 42 mice underwent the surgery to induce postmenopausal osteoporosis. The dorsal midline skin was shaved on all mice. The shaved skin was longitudinally incised, and either the bilateral ovaries were removed or a sham operation was done. Exposed skin and muscle
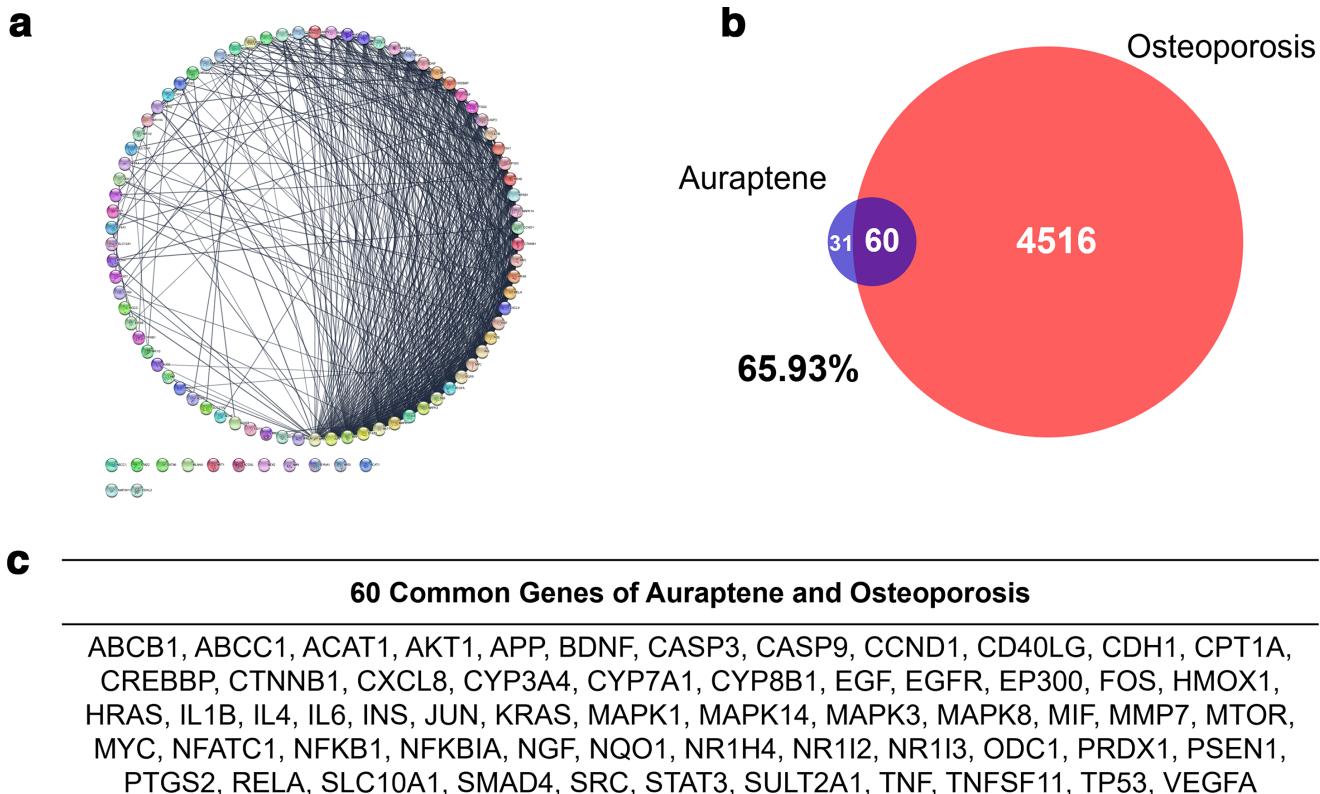
a

b

c

60 Common Genes of Auraptene and Osteoporosis
ABCB1, ABCC1, ACAT1, AKT1, APP, BDNF, CASP3, CASP9, CCND1, CD40LG, CDH1, CPT1A, CREBBP, CTNNB1, CXCL8, CYP3A4, CYP7A1, CYP8B1, EGF, EGFR, EP300, FOS, HMOX1, HRAS, IL1B, IL4, IL6, INS, JUN, KRAS, MAPK1, MAPK14, MAPK3, MAPK8, MIF, MMP7, MTOR, MYC, NFATC1, NFKB1, NFKBIA, NGF, NQO1, NR1H4, NR1I2, NR1I3, ODC1, PRDX1, PSEN1, PTGS2, RELA, SLC10A1, SMAD4, SRC, STAT3, SULT2A1, TNF, TNFSF11, TP53, VEGFA

Fig. 1

a) Network of auraptene (AUR) with 91 nodes and 630 edges. b) Venn diagram of intersection targets between AUR network and the gene sets of osteoporosis disease. c) Common genes of AUR and osteoporosis.

were closed with silk 4-0 suture (AILEE co., South Korea) and povidone-iodine applied to the surgical area to disinfect the skin. After 12 weeks for inducing osteoporosis, the ovariectomized (OVX)-mice were randomly divided into five groups (n = 7): the OVX mice as a negative control group (OVX); the OVX mice treated with 10 µg/kg of 17β-estradiol as a positive control group (E2); and the OVX mice treated with 0.01, 0.1, and 1 mM of AUR (AUR 0.01, 0.1, and 1). AUR (Cat. No. #A9861) and 17β-estradiol (E2) (Cat. No. #E2758) were purchased from MilliporeSigma (USA). Next, 1 mM stock solution of AUR was prepared in dimethyl sulfoxide and dissolved in saline. Then 100 µl of the sample per mouse was intraperitoneally injected once a day for five days per week. Sample administration lasted for four weeks. To check the condition of the mice, body weight was measured every week during the experiments; the mice experienced no adverse effects from the AUR administration. All of the experiments were performed according to the guidelines of the Guide for the Care and Use of Laboratory Animals of the National Institutes of Health,[19] and approved by the Committee on Care and Use of Laboratory Animals of Kyung Hee University (South Korea). We have included an ARRIVE checklist to show that we conformed to the ARRIVE guidelines.

Analysis of the bone minerals. All of the mice were killed under anaesthesia with an intraperitoneal injection of rompun (Elanco Korea, South Korea) after administration of AUR for four weeks. The whole body of each mouse was scanned using DXA followed by dissection of the bone tissues, including the tibia, femur, and lumbar vertebrae (LV). The value was indicated by g/cm^2 for BMD and g for bone mineral content (BMC).

Analysis of the bone microstructure. The excised left femora were fixed with 10% neutralized formalin for 24 hours. Femora were washed in distilled water and demineralized in 0.1 M ethylenediaminetetraacetic acid for two weeks. To process the embedded tissues, the decalcified tissues were dehydrated in ethanol at gradient concentrations and immersed in xylene for two hours each. All samples were embedded in paraffin and consolidated at -20°C for adjusting the hardness between the paraffin and demineralized femora. Paraffin blocks were sectioned at a 7 µm thickness. Femur sections were stained with haematoxylin and eosin (H&E) to examine the bone microstructure and activity of osteoblasts, respectively. Multi-nuclei osteoclasts in the bone marrow of the femoral body (n = 7) were stained by tartrate-resistant acid phosphatase (TRAP) according to the manufacturer's instruction (MilliporeSigma). The area of the medullary cavity at the femoral body stained by H&E and TRAP was visualized

Table I. Biological processes related to targets of auraptene using Kyoto Encyclopedia of Genes and Genomes pathway 2020 human and Gene Ontology process.

Category	FDR value	Description	Matched genes	Background genes
KEGG pathways	1.41E-14	Osteoclast differentiation	14	124
GO process	8.92E-06	Regulation of osteoclast differentiation	6	67
	1.22E-05	Osteoclast differentiation	5	38
	0.0026	Osteoclast development	2	7
	0.0354	Regulation of osteoblast differentiation	3	112

FDR, false discovery rate; GO, Gene Ontology; KEGG, Kyoto Encyclopedia of Genes and Genomes.

under bright fields using the Leica Application Suite (LAS) Microscope Software (Leica Microsystems, USA).

Analysis of serum biomarkers. Blood samples were collected by cardiac puncture under anaesthesia before the kill. The supernatant of the blood, the serum, was obtained by centrifugation at 17,000 rpm for 20 minutes and kept at -20°C until use. The total alkaline phosphatase (ALP), bone-specific alkaline phosphatase (bALP) (AnaSpec, USA), osteocalcin (TaKaRa Bio, Japan), calcium (Nikken SEIL, Japan), and C-telopeptide type I collagen (CTX) (MyBioSource, USA) (n = 7) were analyzed by enzyme-linked immunosorbent assay (ELISA) kit. The procedures were conducted according to the manufacturer's instructions.

Immunofluorescence. For immunofluorescence staining, the tissue slides were deparaffinized and incubated with 3% hydrogen peroxide (H_2O_2) to reduce the endogenous peroxidase activities. After blocking in bovine serum albumin, the tissues were incubated with the primary antibodies anti-receptor activator of nuclear factor kappa-B ligand (RANKL) (Abcam, UK) and nuclear factor of activated T cells 1 (NFATc1) (Santa Cruz Biotechnology, USA) at 4°C overnight. Secondary fluorescent antibodies were incubated in the slides at room temperature, and then the sections were stained with Topro3 dye (BD Biosciences, USA) to counterstain the nucleus. The images of the double-stained tissues were monitored under fluorescence microscopy (Olympus IX71; Olympus, Japan).

Analysis of bone-specific markers by reverse transcription-polymerase chain reaction. The excised LV 4-6 regions (n = 7, respectively) were pulverized by liquid nitrogen to isolate the total RNA and incubated in TRIzol reagent overnight at 4°C to homogenize the bone tissues. Chloroform was added to the homogenized bone tissues to separate the fractions. The supernatants were mixed thoroughly with one volume of 2-propanol to precipitate the RNA pellets. The pellets were washed with 70% (volume/volume (v/v)) ethanol and air-dried. Total RNA pellets were dissolved in RNase free water. Complementary DNA (cDNA) was synthesized from 1 µg of RNA from the bone tissues using the Maxime RT premix kit (Invitrogen, Thermo Fisher Scientific, USA). cDNA was amplified by specific primers using the Maxime PCR premix kit (Invitrogen, Thermo Fisher Scientific). RANKL, NFATc1, dendritic cell specific transmembrane protein (DC-STAMP), cathepsin K (CTS-K), TRAP, matrix metalloproteinase (MMP)-2, MMP-9, and vacuolar-type

H^+-ATPase (V-ATPase) were amplified. The amplification programme started with a pre-denaturation of 94°C for five minutes, followed by 35 cycles that consisted of denaturation at 94°C for 30 seconds, annealing at 55°C to 65°C for one minute and extension at 72°C for two minutes, and ended with heating at a temperature of 72°C for seven minutes and cooling at 4°C. The expression of each product was separated by 1.5% agarose gel and visualized by a unified gel documentation system (Daihan Scientific, South Korea). The bands were normalized to glyceraldehyde 3-phosphate dehydrogenase (GAPDH).
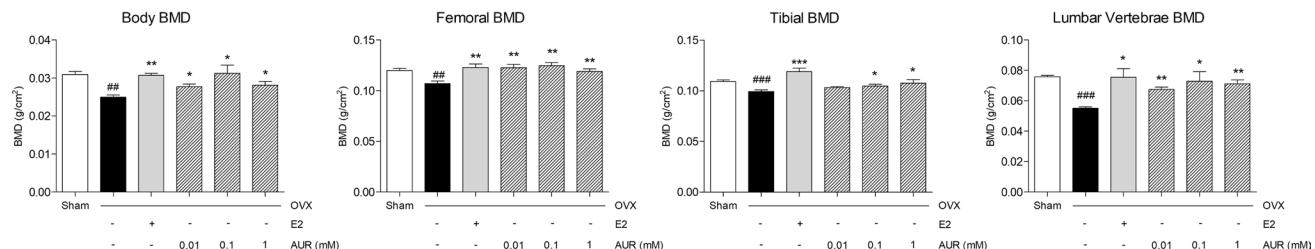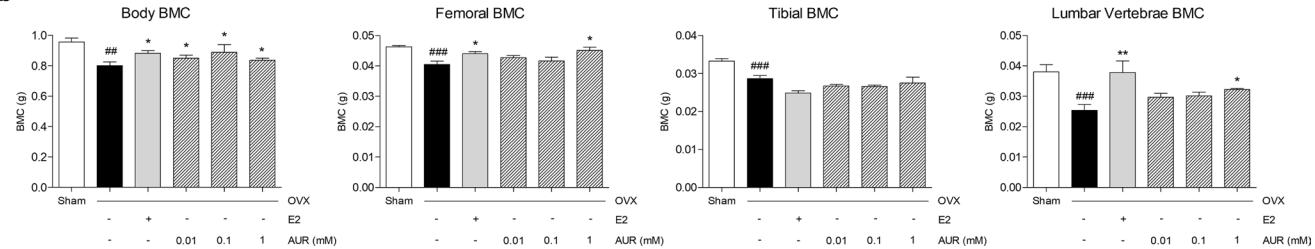
Statistical analysis. Statistical significance was determined by one-way analysis of variance (ANOVA) and Tukey multiple comparison tests using SPSS Data Analysis Version 17.0 (SPSS, USA). In all the analyses, $p < 0.05$ was taken to indicate statistical significance.

Results

Investigation of the association of AUR and osteoporosis through network construction. A total of 91 genes were yielded as chemical-gene co-occurrences of AUR. A network of AUR was constructed with 91 nodes and 630 edges (Figure 1a). The target genes of AUR were 91 and those of osteoporosis disease were 4,576. The Venn diagram of AUR targets and osteoporosis targets showed that 60 identical targets were obtained as common genes. Approximately 65.93% of the total target genes of AUR matched to the target genes of osteoporosis (Figure 1b). The crossover genes of AUR and osteoporosis are listed in Figure 1c.

Prediction of potential pathway by enrichment analysis of KEGG and GO of the target genes of AUR. To predict the potential pathway of AUR on osteoporosis, the terms related to osteoporosis were sorted in the enriched pathways derived from AUR (Table I). Among those pathways, 'osteoclast differentiation' in the KEGG pathways were assigned to be a predicted underlying mechanism of AUR. In addition, GO process terms including 'Regulation of osteoclast differentiation', 'Osteoclast differentiation', 'Osteoclast development', and 'Regulation of osteoblast differentiation' were shown with false discovery rate (FDR) value < 0.05.

Effects of AUR on BMC and BMD in OVX-induced mice. To determine the changes of the inorganic mineral content in the bone, BMC and BMD were measured. In Figure 2a, the OVX group showed that BMC was decreased compared to the sham group in the whole body, femur, tibia,

Fig. 2

Effects of auraptene (AUR) on: a) bone mineral density (BMD); and b) bone mineral content (BMC). BMD and BMC levels were measured in total body, femur, tibia, and lumbar vertebrae (LV). Results are presented as mean (standard error of the mean). ##p < 0.01 and ###p < 0.001 versus Sham group; *p < 0.05, **p < 0.01, and ***p < 0.001 versus ovariectomized (OVX) group. E2, 17β-estradiol group.

and LV. Treatment of E2 increased the BMC compared to the OVX group in the whole body, femur, and LV by 10.21%, 8.62%, and 49.11%, respectively. In addition, the BMC of the whole body, femur, and LV were increased by 4.46%, 11.26%, and 26.90%, respectively, in the treatment with AUR 1 mM. However, there were no effects of AUR on the tibial BMC. As with the BMC, the BMD levels were decreased in the OVX group compared to the sham group. The E2 treatment significantly increased the BMD levels in the whole body (p = 0.010), femur (p = 0.001), tibia (p = 0.001), and LV (p = 0.006) by 23.02%, 14.66%, 19.80%, and 37.15%, respectively. The AUR 1 mM treatment increased the BMD in the whole body, femur, tibia, and LV by 12.61%, 11.11%, 8.43%, and 29.22%, respectively (Figure 2b).

Effects of AUR on bone microstructure in the OVX-induced mice. The extension of the bone medullary cavity changed the bone microstructure and reduced the collagen deposition in the OVX group compared with the sham group. However, the femoral shafts were filled with bone marrow in the medullary cavity when treated with E2 and AUR. In particular, the AUR treatment dose-dependently filled the medullary cavity with bone marrow (Figure 3a).

Effects of AUR on bone-specific markers in the serum. As shown in Figure 3b, ALP and bALP were decreased in the OVX group compared to the sham group by 26.03% and 40.55%, respectively. Treatment of E2 upregulated the expression levels of ALP and bALP by 24.52% and 24.74%, respectively, compared to the OVX group. In addition, the AUR 1 mM treatment markedly increased the secretion of ALP and bALP by 27.54% and 33.65%, respectively, compared to the OVX group. Similarly, the osteocalcin and calcium levels were decreased by

38.77% and 31.07%, respectively, in the OVX group compared to sham group, while the E2 treatment upregulated the expression levels of osteocalcin and calcium by 46.65% and 57.26%, respectively, compared to the OVX group. Administration of AUR 1 mM improved the production of osteocalcin and calcium by 38.74% and 82.90%, respectively. Moreover, serum CTX level was 3.01-times increased in the OVX mice compared to Sham mice. Treatment with AUR at 0.01 mM, 0.1 mM, and 1 mM concentrations significantly reduced serum CTX levels by 25.35% (p = 0.003), 28.80% (p = 0.001), and 29.05% (p = 0.001), respectively.

Effects of AUR on TRAP-stained osteoclast activity in femoral bone tissues. OVX in mice markedly increased the osteoclastic activity in the bone marrow of bone tissues compared to the Sham group. Treatment with 0.01, 0.1, and 1 mM of AUR induced decreases in the number of osteoclasts in the femoral body stained by TRAP staining (Figure 4). In particular, 1 mM of AUR apparently recovered the osteoclast activity in the bone marrow of the bone tissues similar to the Sham group.

Effects of AUR on RANKL+NFATc1+ expressions in the femoral bone tissues. OVX-induced osteoporotic bone tissues showed increases of RANKL+NFATc1+ expressions. As the immunofluorescence staining showed, expression of RANKL+NFATc1+ was markedly increased in the femoral body of the OVX group, compared to the Sham group. By treatment with AUR at all concentrations, the fluorescent intensities of the RANKL and NFATc1 probe were weaker than that in the osteoporotic bone tissues (Figure 5).

Effects of AUR on osteoclastic mediators including RANKL, NFATc1, TRAP, and DC-STAMP in the bone tissues. The messenger RNA (mRNA) expressions of RANKL, NFATc1,
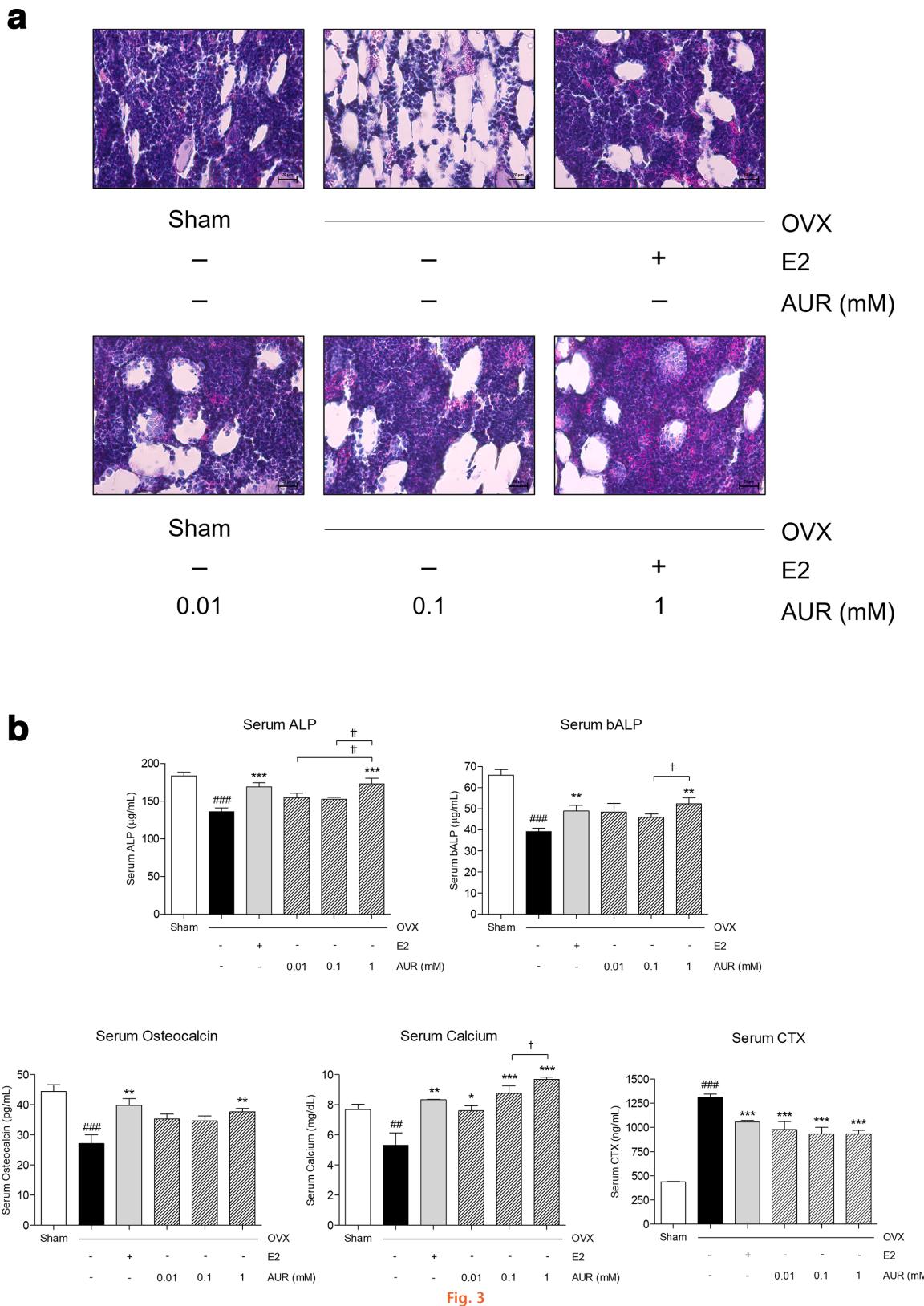
Fig. 3

a) Effects of auraptene (AUR) on bone marrow in ovariectomized (OVX)-induced mice. Representative images of haematoxylin and eosin staining for measuring histomorphometrical changes of femur (magnification 400×, scale bar = 10 μm). b) Effects of AUR on serum alkaline phosphatase (ALP), bone-specific alkaline phosphatase (bALP), osteocalcin, calcium, and C-telopeptide type I collagen (CTX) in OVX-induced mice. Results are presented as mean (standard error of the mean) (n = 7). $^{##}p < 0.01$ and $^{###}p < 0.001$ versus Sham group; $^{*}p < 0.05$, $^{**}p < 0.01$, and $^{***}p < 0.001$ versus OVX group; $†p < 0.05$, $††p < 0.01$ versus experimental groups (AUR 0.01, AUR 0.1, and AUR 1). E2, 17β-estradiol group.

Fig. 4

Effects of auraptene (AUR) on tartrate-resistant acid phosphatase (TRAP)-positive osteoclasts in the bone marrow of femoral body in ovariectomized (OVX)-induced mice. Representative images of TRAP staining for measuring osteoclast activities in femur (magnification 200×, scale bar = 20 μm). Yellow arrows indicate the TRAP-positive osteoclasts. E2, 17β-estradiol group.

TRAP, and DC-STAMP were increased by 2.8 times, 4.7 times, 1.3 times, and 2.7 times in the OVX group, respectively, compared to the Sham group. Treatment of E2 decreased the expression levels of RANKL, NFATc1, TRAP, and DC-STAMP by 59.8%, 58.7%, 58.3%, and 45.7% in the OVX-induced osteoporotic mice. By administration of AUR 0.01, 0.1, and 1 mM, the RANKL expression level was decreased by 55.7%, 62.9%, and 79.2%, respectively, in a dose-dependent manner. All concentrations (0.01, 0.1, and 1 mM) of AUR significantly decreased the expression level of NFATc1 by 66.3% ($p = 0.012$), 67.3% ($p = 0.011$), and 77.2% ($p = 0.006$), respectively (Figure 6a). In addition, the increased expression level of TRAP in osteoporotic bone tissues was significantly reduced by 0.1 mM ($p = 0.003$) and 1 mM of AUR ($p = 0.001$) (Figure 6b). Furthermore, DC-STAMP expression level was decreased to 37.6%, 50.7%, and 81.7% compared to the OVX group in a dose-dependent manner (Figure 6c).

Effects of AUR on osteoclastic mediators regarding the bone matrix degradation including CTS-K, MMP-9, V-ATPase d2, and V-ATPase a3 in the bone tissues. Messenger RNA expression levels of CTS-K, MMP-9, V-ATPase d2,

and V-ATPase a3 in the OVX group were upregulated to 1.8-fold, 4.1-fold, 3.5-fold, and 3.2-fold, respectively, compared to Sham group. E2 treatment downregulated the expressions of those markers in the bone tissues by 40.0%, 76.5%, 31.1%, and 27.4%, respectively, in comparison to the OVX group. The 1 mM AUR treatment significantly ($p = 0.001$) downregulated the expression of CTS-K by 73.9% in the bone tissues. In addition, MMP-9 mRNA expression levels were decreased to 52.1% by 1 mM of AUR (Figure 7a). Moreover, treatment with AUR 0.01, 0.1, and 1 mM significantly ($p = 0.001$) reduced the levels of V-ATPase d2 and V-ATPase a3 in the bone tissues compared to the OVX group (Figure 7b).

Discussion

Osteoporosis is a common bone disease, making the bone weak and brittle because of the bigger spaces in the honeycomb structure.[20] It leads to a disturbance of the balance of bone cells, osteoblasts, and osteoclasts, resulting in a reduction of bone integrity and induction of bone loss.[21] In elderly women, the activity of osteoclasts as bone-resorbing cells is predominant compared
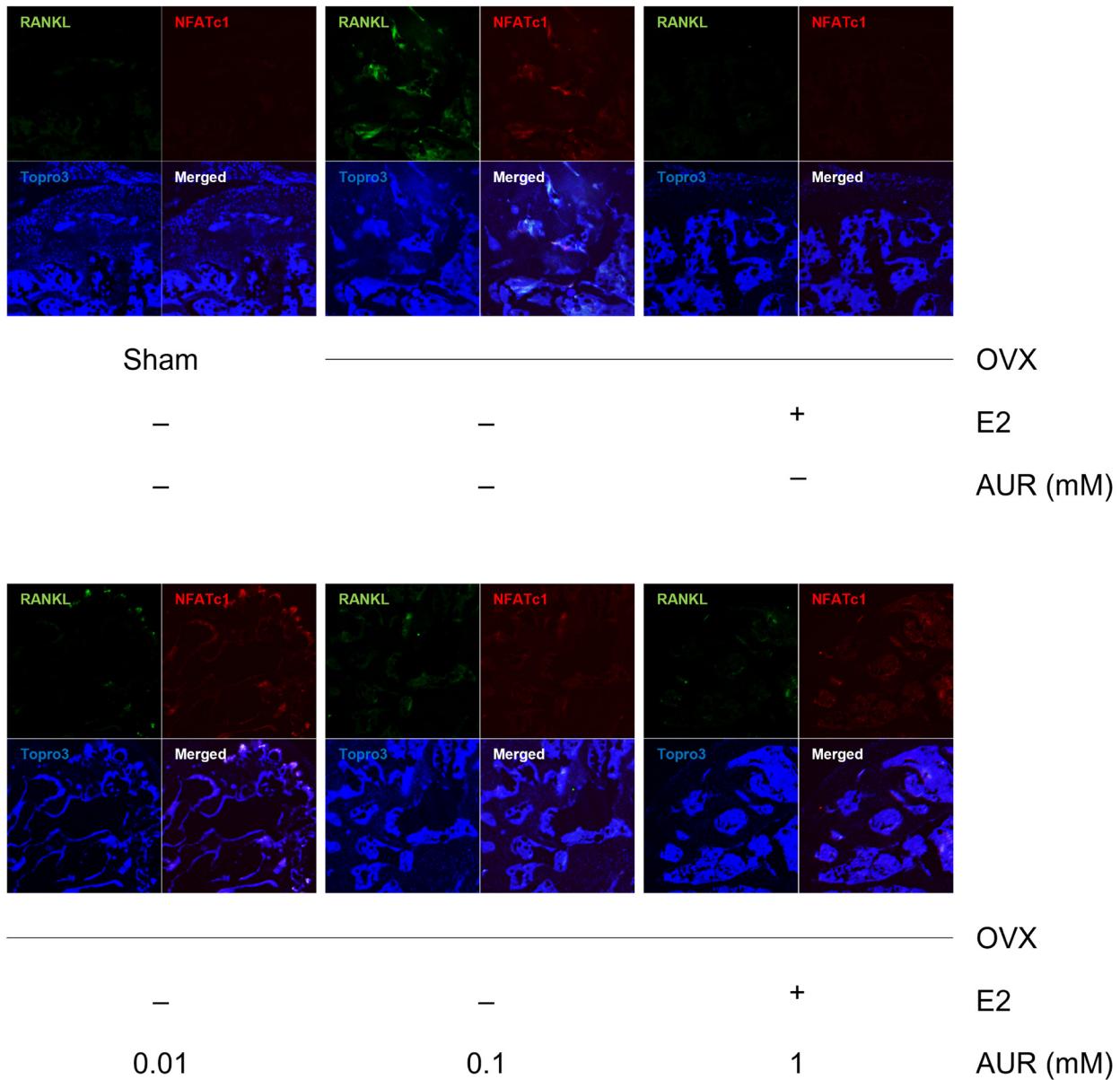
Fig. 5

Effects of auraptene (AUR) on receptor activator of nuclear factor kappa-B ligand (RANKL)+nuclear factor of activated T cells 1 (NFATc1)+ expressions in the femoral body in ovariectomized (OVX)-induced mice (magnification 200×, scale bar = 20 µm). Green, RANKL; Red, NFATc1; Blue, Topro3. E2, 17β-estradiol group.

to the activation of osteoblasts as bone formation cells, due to the rapid decline in oestrogen concentration.[22,23] Assessment of BMD has been known to be an important diagnostic marker for osteoporosis, because bone loss occurs without symptoms.[24] In this study, we analyzed the relevance of possible effects and potential molecular pathways of AUR on osteoporosis using network pharmacology. The network of AUR had 91 nodes and 630 edges. In total, 65.93% of the target genes in the AUR network were overlapped with the 4,576 osteoporosis-related genes, indicating that the potential efficacy of AUR is closely associated with osteoporosis disease. Based on the predicted results, the BMD and BMC levels were measured in the bone tissues of OVX-induced mice including the whole body, femora, tibia, and lumbar spine to evaluate the effects of AUR on osteoporosis. OVX dropped off the levels of bone minerals, while the AUR treatment markedly improved the levels of BMD and BMC
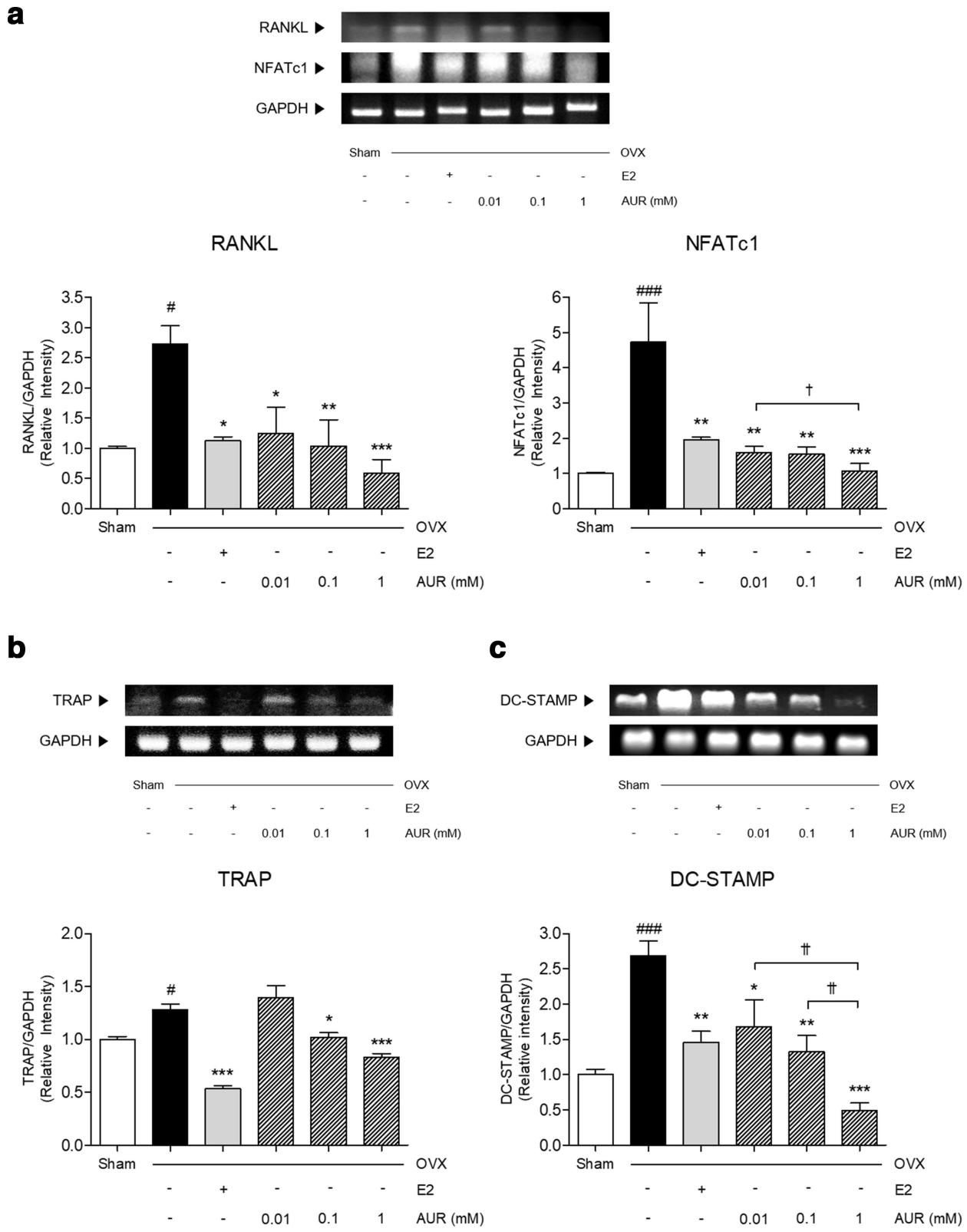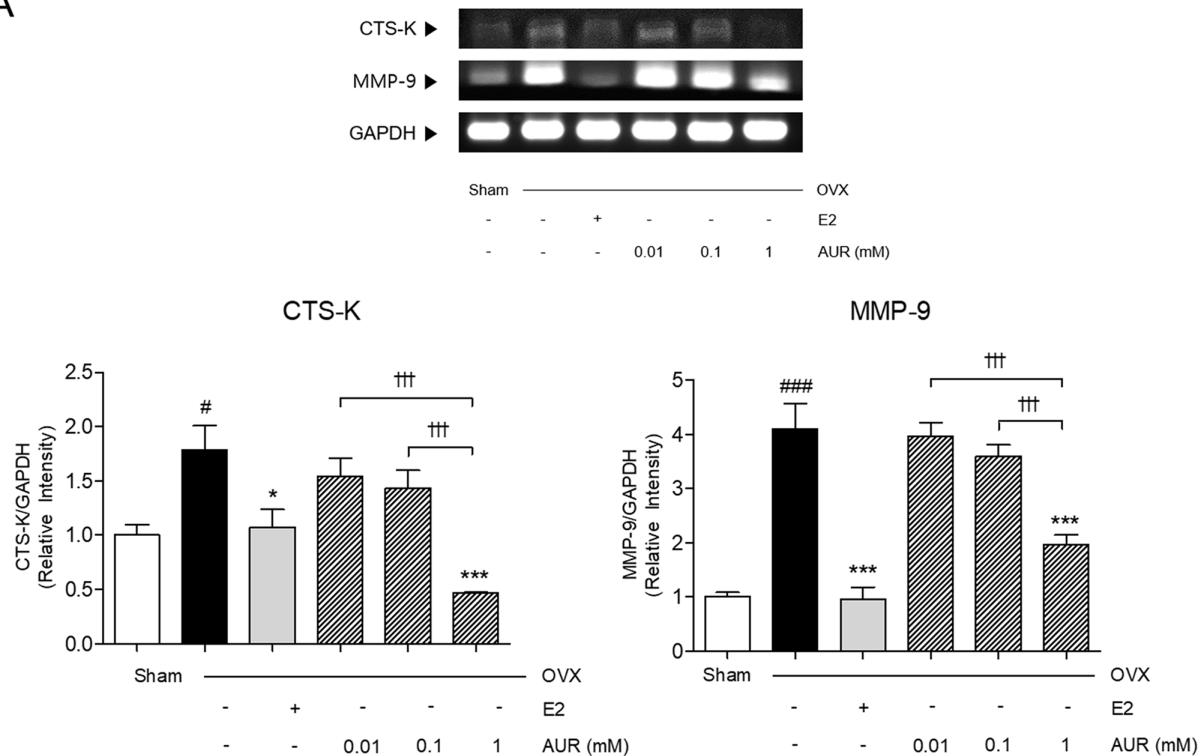
a

b

c

Fig. 6

Effects of auraptene (AUR) on the messenger RNA (mRNA) expression levels of osteoclastic markers including: a) receptor activator of nuclear factor kappa-B ligand (RANKL) and nuclear factor of activated T cells 1 (NFATc1); b) tartrate-resistant acid phosphatase (TRAP); and c) DC-STAMP in femur (n = 7). Results are presented as mean (standard error of the mean). ##p < 0.01 and ###p < 0.001 versus Sham group; *p < 0.05, **p < 0.01, and ***p < 0.001 versus ovariectomized (OVX) group; †p < 0.05, ††p < 0.01 versus experimental groups (E2, AUR 0.01, AUR 0.1, and AUR 1). DC-STAMP, dendritic cell-specific transmembrane protein; E2, 17β-estradiol group; GAPDH, glyceraldehyde 3-phosphate dehydrogenase.
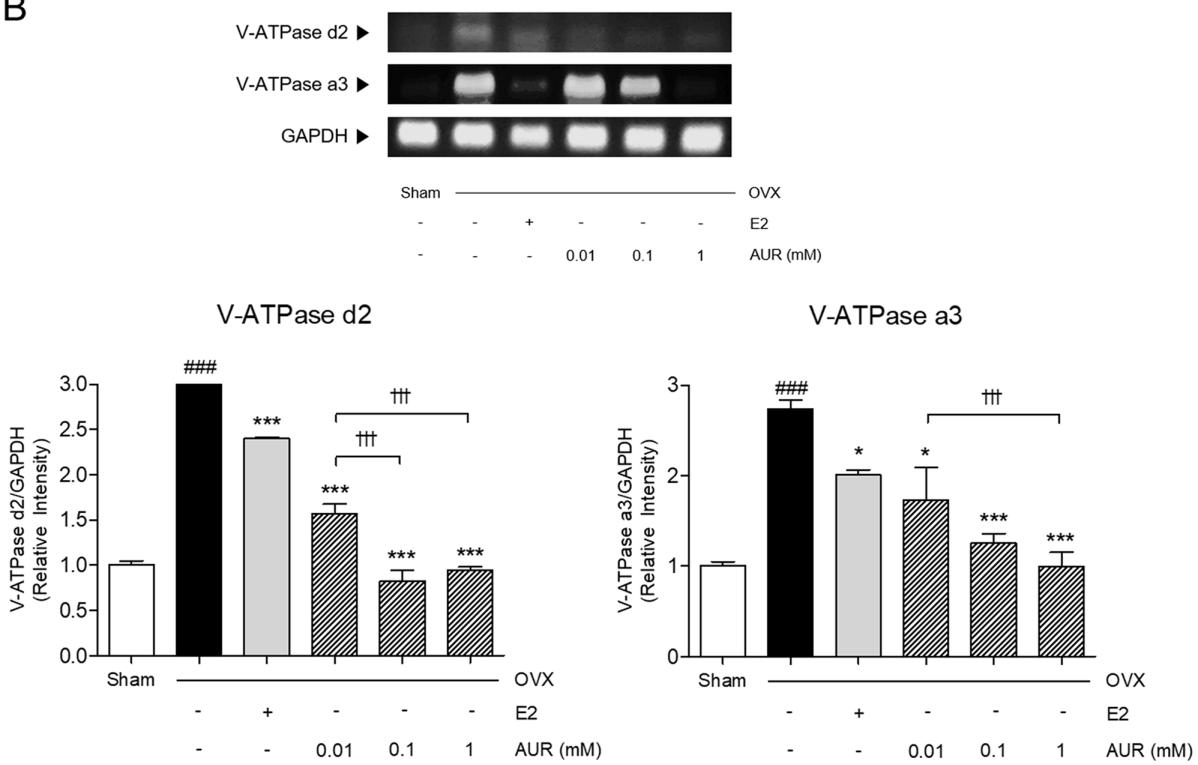
Fig. 7

Effects of auraptene (AUR) on the messenger RNA (mRNA) expression levels of osteoclastic markers including: a) cathepsin K (CTS-K) and matrix metalloproteinase (MMP)-9; and b) vacuolar ATPase (V-ATPase) d2 and V-ATPase a3 in femur (n = 7). Results are presented as mean (standard error of the mean). ##$p < 0.01$ and ###$p < 0.001$ versus Sham group; *$p < 0.05$, **$p < 0.01$, and ***$p < 0.001$ versus ovariectomized (OVX) group; †††$p < 0.001$ versus experimental groups (E2, AUR 0.01, AUR 0.1, and AUR 1). E2, 17β-estradiol group; GAPDH, glyceraldehyde 3-phosphate dehydrogenase.
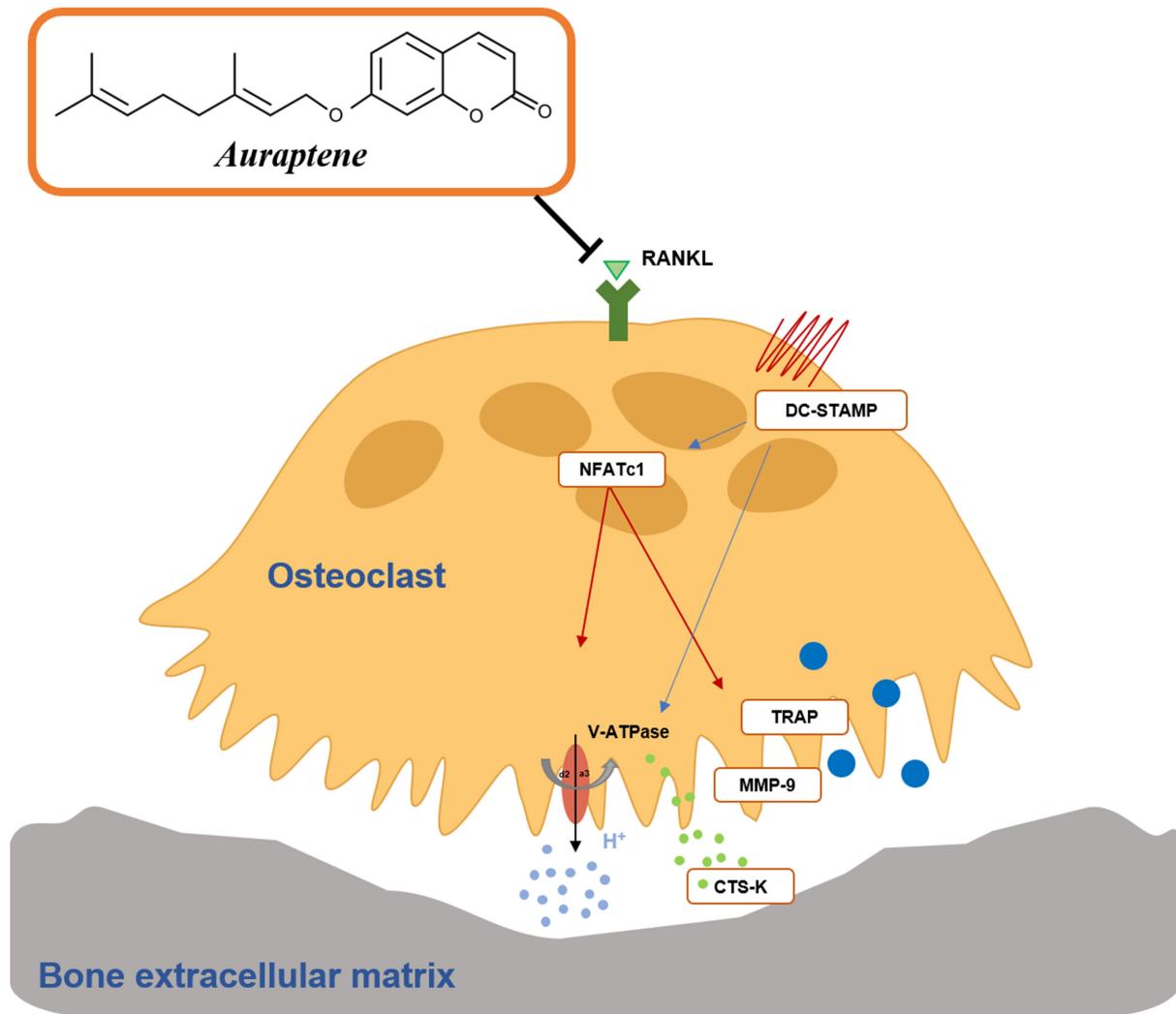
Fig. 8

Schematic diagram of auraptene (AUR) on osteoporosis. CTS-K, cathepsin K; DC-STAMP, dendritic cell-specific transmembrane protein; MMP, matrix metalloproteinase; NFATc1, nuclear factor of activated T cells 1; RANKL, receptor activator of nuclear factor-κB ligand; TRAP, tartrate-resistant acid phosphatase; V-ATPase, vacuolar ATPase.

in the whole body, femora, tibia, and lumbar spine in OVX-induced osteoporotic mice. Accompanying changes in the mineral contents and changes in the bone architecture, which is a clinical manifestation of osteoporosis, affect the bone quality. Expansion of bone marrow adipocytes is commonly observed in osteoporosis. Adipose-rich bone marrow contributes to the decrease of the trabecular bone volume.[25] According to the correlation between the BMD and bone histological structure, the progression of osteoporosis can be estimated by determining cellular pathophysiology. It is well established that there is a honeycomb-like structure filled with the bone marrow in the OVX-induced osteoporotic mice.[26] The AUR treatment recovered the bone histological structure, especially reduction of adipocyte size in the bone marrow cells of the femur. Taken together, the effects of

AUR on bone integrity were confirmed by assessment of the BMD level and the bone architecture.

Serum ALP, bALP, osteocalcin, and calcium as secondary diagnostic markers for osteoporosis are secreted under the condition of bone loss.[1] ALP is regarded as a predictor of bone loss in post-menopausal osteoporotic females.[27] In particular, bALP plays an important role in activation of osteoblasts.[28] Osteocalcin, released from osteoblasts, plays a role in bone mineralization.[29] Additionally, calcium is a key component of the bone extracellular matrix for the maintenance of healthy bones.[30] Administration of AUR increased the levels of the total serum ALP and bALP in osteoporotic mice. In addition, the osteocalcin and calcium concentrations in the serum were recovered by the AUR treatment. Furthermore, serum CTX concentration has been regarded as a marker of osteoclast activity.

Increase of CTX level may predict the risk of bone resorption by osteoclast.[27] AUR treatment markedly decreased the level of CTX in serum. Taken together, the results that the BMD levels and the concentrations of the serum diagnostic markers, including ALP, bALP, osteocalcin, calcium, and CTX, were recovered by AUR showed the effects of AUR on inhibition of bone loss in osteoporosis.

There is available evidence showing that the effects of AUR on osteoporosis are closely related to the inhibition of osteoclast activity.[16] In our previous research, *Zanthoxylum piperitum* containing AUR ameliorated osteoporosis by inhibiting osteoclast differentiation. Additionally, an AUR derivative is reported to suppress osteoclast differentiation by inhibiting mitogen-activated protein kinase and c-Fos/NFATc1.[15] In addition to the previous literature, underlying pathway of AUR on osteoporosis was predicted from enrichment analysis including the KEGG pathway and GO terms. As a result of classifying the biological terms associated with osteoporosis in the whole enrichment analysis, 'osteoclast differentiation' or 'osteoclast development' was found as a relevant pathway. Furthermore, serum CTX, a biochemical marker of osteoporosis activation, was markedly reduced by AUR treatment in the present study. Based on the previous reports, prediction result, and serum CTX data, the underlying mechanism of AUR for osteoporosis was clarified in the field of inhibition of osteoclast-mediated bone resorption. We found that AUR treatment markedly inhibited the TRAP-positive osteoclast activities in the bone marrow of the femur. In the process of bone resorption, consecutive events occur: osteoclastogenesis from osteoclast precursor cells; and attachment of osteoclasts to the matrix and degradation of the bone matrix by mature osteoclasts.[31] At the initial phase, binding of RANKL to the receptor activator of nuclear factor kappa-B (RANK) directly triggers osteoclast differentiation from osteoclast precursor cells to osteoclasts. For osteoclast differentiation, RANKL activates NFATc1, which is downstream of the RANKL-RANK signalling pathway in osteoclasts as a transcription factor.[32] DC-STAMP is a key regulator of the cell fusion of osteoclasts controlled by NFATc1.[33] Then, osteoclasts attach to the bone matrix containing type 1 collagen and noncollagenous proteins.[34] In the process of mature osteoclast-mediated bone resorption, transcription of NFATc1 upregulates the release of osteoclast-related genes including CTS-K, TRAP, and MMP-9.[32] TRAP is produced by only bone-resorbing osteoclasts, and therefore is considered to be a key indicator of bone erosion.[35] In addition, TRAP is able to dephosphorylate the bone matrix proteins, which are synthesized by the inactive proenzyme.[36] CTS-K and MMP-9 as proteases initiate the osteoclastic resorption and degrade collagenous or non-collagenous bone matrix.[37,38] V-ATPases, protein complexes of ATP hydrolysis on the cell membrane, are important in acidification of the bone extracellular matrix for bone resorption.[39] Specifically, subunit d2 and a3 of V-ATPase have been demonstrated to be involved in the osteoclast function as a major proton pump.[40] In our study, AUR attenuated the levels of osteoclastic genes that had been raised by OVX. AUR decreased RANKL expression in bone tissues, resulting in the inhibition of osteoclast differentiation and the initiation of NFATc1 transcription. Excessive expressions of RANKL$^+$NFATc1$^+$ indicated by immunofluorescence staining were apparently decreased by the AUR treatment. TRAP is known as an indicator of osteoclasts and a marker of cell fusion.[36] We suggested that AUR treatment abrogated the cell fusion as well as mature osteoclast formation through the results from decrease of TRAP-osteoclasts by AUR in the OVX-induced osteoporotic mice. Additionally, various factors involved in the degradation of the extracellular bone matrix were decreased by the AUR treatment. AUR reduced the mRNA expressions of proteases (CTS-K and MMP-9) and acidification pumps (V-ATPase d2 and V-ATPase a3) in the bone tissues. Taken together, those results suggest that AUR might be related to the inhibition of RANKL/NFATc1 signalling pathway-mediated bone resorption according to the results below. There were apparent reductions of RANKL and NFATc1 expressions in the AUR-treated bone tissues. Following AUR-induced NFATc1 inactivation, DC-STAMP, a cell fusion marker to form multinucleated osteoclasts, was decreased. Next, bone erosion was effectively blocked during the process of the degradation of collagenous or non-collagenous bone matrix and the acidification of the bone extracellular matrix by inhibiting the RANKL/NFATc1 pathway upon the AUR treatment. These findings lead to the involvement of RANKL/NFATc1-mediated mechanisms by which AUR inhibited bone osteoclastic resorption. In summary, AUR inhibited osteoclast-mediated bone resorption by attenuating osteoclast differentiation to mature osteoclasts and the degradation of the bone matrix (Figure 8).

In conclusion, AUR ameliorated bone loss in osteoporosis by suppression of osteoclast activities. Approximately 65.93% of the target genes derived from AUR were matched with osteoporosis-related genes. Through enrichment analysis, osteoclast differentiation was predicted to be a potential molecular pathway of AUR. AUR increased the BMD levels in the whole body, femora, tibia, and lumbar spine, and improved the histological structure in the osteoporotic bone, leading to the restoration of bone integrity. Serum biomarkers including ALP, bALP, osteocalcin, and calcium were increased by the AUR administration. TRAP-positive osteoclast activities were reduced by the AUR treatment. The underlying mechanism of AUR on osteoporosis is closely associated with the inhibition of osteoclast differentiation and the degradation of the bone matrix through the RANKL/NFATc1 pathway. Consequently, AUR is anticipated to be helpful for treating osteoporosis.

Supplementary material

Table showing the coefficient genes of auraptene obtained from PubChem. An ARRIVE checklist is also included to show that the ARRIVE guidelines were adhered to in this study.

References

1. **Lane NE**. Epidemiology, etiology, and diagnosis of osteoporosis. *Am J Obstet Gynecol*. 2006;194(2 Suppl):S3-11.
2. **Lips P**, **van Schoor NM**. Quality of life in patients with osteoporosis. *Osteoporos Int*. 2005;16(5):447–455.
3. **Sözen T**, **Özışık L**, **Başaran NÇ**. An overview and management of osteoporosis. *Eur J Rheumatol*. 2017;4(1):46–56.
4. **Ström O**, **Borgström F**, **Kanis JA**, **et al**. Osteoporosis: burden, health care provision and opportunities in the EU. *Arch Osteoporos*. 2011;6(1–2):59–155.
5. **Blake GM**, **Fogelman I**. The role of DXA bone density scans in the diagnosis and treatment of osteoporosis. *Postgrad Med J*. 2007;83(982):509–517.
6. **Solomon CG**, **Black DM**, **Rosen CJ**. Postmenopausal osteoporosis. *N Engl J Med*. 2016;374(3):254–262.
7. **Akkawi I**, **Zmerly H**. Osteoporosis: current concepts. *Joints*. 2018;6(2):122–127.
8. **Rosen CJ**. The Epidemiology and Pathogenesis of Osteoporosis. In: Feingold KR, Anawalt B, Boyce A, et al, eds. *Endotext [Internet]*. South Dartmouth, Massachusetts: MDText.com, Inc, 2000.
9. **Tang CH**. Osteoporosis: from molecular mechanisms to therapies. *Int J Mol Sci*. 2020;21(3):714.
10. **Tsai KS**. Encouraging appropriate osteoporosis medication to prevent fracture. *Osteoporos Sarcopenia*. 2016;2(3):117.
11. **Sieber P**, **Lardelli P**, **Kraenzlin CA**, **Kraenzlin ME**, **Meier C**. Intravenous bisphosphonates for postmenopausal osteoporosis: safety profiles of zoledronic acid and ibandronate in clinical practice. *Clin Drug Investig*. 2013;33(2):117–122.
12. **Derosa G**, **Maffioli P**, **Sahebkar A**. Aurapten and its role in chronic diseases. *Adv Exp Med Biol*. 2016;929:399–407.
13. **Bibak B**, **Shakeri F**, **Barreto GE**, **Keshavarzi Z**, **Sathyapalan T**, **Sahebkar A**. A review of the pharmacological and therapeutic effects of auraptene. *Biofactors*. 2019;45(6):867–879.
14. **Abdallah BM**, **Ali EM**. 5′-hydroxy auraptene stimulates osteoblast differentiation of bone marrow-derived mesenchymal stem cells via a BMP-dependent mechanism. *J Biomed Sci*. 2019;26(1):51.
15. **Abdallah BM**, **Ali EM**, **Elsawy H**, **Badr GM**, **Abdel-Moneim AM**, **Alzahrani AM**. The coumarin derivative 5′-hydroxy auraptene suppresses osteoclast differentiation via inhibiting MAPK and c-Fos/NFATc1 pathways. *Biomed Res Int*. 2019;2019:9395146.
16. **Kim MH**, **Lee H**, **Ha IJ**, **Yang WM**. Zanthoxylum piperitum alleviates the bone loss in osteoporosis via inhibition of RANKL-induced c-fos/NFATc1/NF-kappaB pathway. *Phytomedicine*. 2021;80:153397.
17. **No authors listed**. PubChem. National Library of Medicine. 2022. https://pubchem.ncbi.nlm.nih.gov/ (date last accessed 20 April 2022).
18. **No authors listed**. GeneCards®: The Human Gene Database. Weizmann Institute of Science. 2022. http://www.genecards.org/ (date last accessed 20 April 2022).
19. **No authors listed**. *Guide for the Care and Use of Laboratory Animals*. Eighth ed. Washington, D.C: The National Academies Press, 2011.
20. **Elbossaty WF**. Mineralization of bones in osteoporosis and osteomalacia. *Ann Clin Lab Res*. 2017;5(4):201.
21. **Noor Z**, **Sumitro SB**, **Hidayat M**, **Rahim AH**, **Sabarudin A**, **Umemura T**. Atomic mineral characteristics of Indonesian osteoporosis by high-resolution inductively coupled plasma mass spectrometry. *ScientificWorldJournal*. 2012;2012:372972.
22. **Drake MT**, **Clarke BL**, **Lewiecki EM**. The pathophysiology and treatment of osteoporosis. *Clin Ther*. 2015;37(8):1837–1850.
23. **Nicholson T**, **Scott A**, **Newton Ede M**, **Jones SW**. Do E-cigarettes and vaping have a lower risk of osteoporosis, nonunion, and infection than tobacco smoking? *Bone Joint Res*. 2021;10(3):188–191.
24. **Kim JH**, **Seo BK**, **Baek YH**. Quality assessment of traditional and conventional medicine clinical practice guidelines for osteoporosis. *Medicine (Baltimore)*. 2021;100(5):e24559.
25. **Pino AM**, **Rosen CJ**, **Rodríguez JP**. In osteoporosis, differentiation of mesenchymal stem cells (MSCs) improves bone marrow adipogenesis. *Biol Res*. 2012;45(3):279–287.
26. **Lei Z**, **Xiaoying Z**, **Xingguo L**. Ovariectomy-associated changes in bone mineral density and bone marrow haematopoiesis in rats. *Int J Exp Pathol*. 2009;90(5):512–519.
27. **Saleh N**, **Nassef NA**, **Shawky MK**, **Elshishiny MI**, **Saleh HA**. Novel approach for pathogenesis of osteoporosis in ovariectomized rats as a model of postmenopausal osteoporosis. *Exp Gerontol*. 2020;137:110935.
28. **Kuo TR**, **Chen CH**. Bone biomarker for the clinical assessment of osteoporosis: recent developments and future perspectives. *Biomark Res*. 2017;5:18.
29. **Park SY**, **Ahn SH**, **Yoo JI**, **et al**. Clinical application of bone turnover markers in osteoporosis in Korea. *J Bone Metab*. 2019;26(1):19–24.
30. **Tariq S**, **Tariq S**, **Lone KP**, **Khaliq S**. Alkaline phosphatase is a predictor of bone mineral density in postmenopausal females. *Pak J Med Sci*. 2019;35(3):749–753.
31. **Teitelbaum SL**. Bone resorption by osteoclasts. *Science*. 2000;289(5484):1504–1508.
32. **Kim JH**, **Kim N**. Regulation of NFATc1 in osteoclast differentiation. *J Bone Metab*. 2014;21(4):233–241.
33. **Choi BY**, **Park CH**, **Na YH**, **Bai HW**, **Cho JY**, **Chung BY**. Inhibition of RANKL-induced osteoclast differentiation through the downregulation of c-Fos and NFATc1 by Eremochloa ophiuroides (centipedegrass) extract. *Mol Med Rep*. 2016;13(5):4014–4022.
34. **Blair HC**, **Kahn AJ**, **Crouch EC**, **Jeffrey JJ**, **Teitelbaum SL**. Isolated osteoclasts resorb the organic and inorganic components of bone. *J Cell Biol*. 1986;102(4):1164–1172.
35. **Bernhardt A**, **Skottke J**, **von Witzleben M**, **Gelinsky M**. Triple culture of primary human osteoblasts, osteoclasts and osteocytes as an in vitro bone model. *Int J Mol Sci*. 2021;22(14):7316.
36. **Solberg LB**, **Brorson SH**, **Stordalen GA**, **Bækkevold ES**, **Andersson G**, **Reinholt FP**. Increased tartrate-resistant acid phosphatase expression in osteoblasts and osteocytes in experimental osteoporosis in rats. *Calcif Tissue Int*. 2014;94(5):510–521.
37. **Logar DB**, **Komadina R**, **Prezelj J**, **Ostanek B**, **Trost Z**, **Marc J**. Expression of bone resorption genes in osteoarthritis and in osteoporosis. *J Bone Miner Metab*. 2007;25(4):219–225.
38. **Zheng X**, **Zhang Y**, **Guo S**, **Zhang W**, **Wang J**, **Lin Y**. Dynamic expression of matrix metalloproteinases 2, 9 and 13 in ovariectomy-induced osteoporosis rats. *Exp Ther Med*. 2018;16(3):1807–1813.
39. **Duan X**, **Yang S**, **Zhang L**, **Yang T**. V-ATPases and osteoclasts: ambiguous future of V-ATPases inhibitors in osteoporosis. *Theranostics*. 2018;8(19):5379–5399.
40. **Matsumoto N**, **Daido S**, **Sun-Wada GH**, **Wada Y**, **Futai M**, **Nakanishi-Matsui M**. Diversity of proton pumps in osteoclasts: V-ATPase with a3 and d2 isoforms is a major form in osteoclasts. *Biochim Biophys Acta*. 2014;1837(6):744–749.

Author information:
- M. H. Kim, PhD, Research Professor
- L. Y. Choi, MS, Student for Master of Science
- J. Y. Chung, BS, Student for Bachelor of Science
- W. M. Yang, KMD, PhD, Professor
  Department of Convergence Korean Medical Science, Graduate School, College of Korean Medicine, Kyung Hee University, Seoul, South Korea.
- E-J. Kim, KMD, PhD, Professor, Department of Acupuncture & Moxibustion, Dongguk University Bundang Oriental Hospital, Seongnam, South Korea.

Author contributions:
- M. H. Kim: Conceptualization, Formal analysis, Investigation, Writing – original draft.
- L.Y. Choi: Investigation, Writing – original draft.
- J. Y. Chung: Investigation, Writing – original draft.
- E-J. Kim: Investigation, Writing – review & editing, Supervision.
- W. M. Yang: Conceptualization, Formal analysis, Investigation, Project administration, Supervision, Writing – original draft.

- E-J. Kim and W. M. Yang contributed equally to this work.